

Comparison of an underground rock face 3D modeling performance: SfM-MVS with optimum photographing settings and LiDAR technology

Junsu Leem

Seoul National University, Seoul, Korea

Jineon Kim

Seoul National University, Seoul, Korea

Jiwon Choi

Seoul National University, Seoul, Korea

Jae-Joon Song

Research Institute of Energy and Resources, Seoul National University, Seoul, Korea

ABSTRACT: Structure-from-motion & multi-view-stereo (SfM-MVS) and light-detecting-and-ranging (LiDAR) are the representative methods to generate a 3D point cloud of a rock face. Both methods have pros and cons depending on the conditions including illumination, surveying time, resolution, accuracy, and cost. For application in underground space, SfM-MVS has been used less than LiDAR due to its lack of error pre-determination and ambiguity of photographing settings. Leem (2023) has developed a theoretical error prediction model for SfM-MVS and derived optimum photographing settings which minimize SfM-MVS error under light and time constraints. This work utilized the optimum photographing settings for the SfM-MVS and compared it with LiDAR when modeling a $70 \leq \nu$ rock face at an illumination of 25 lx within 5 minutes at a tunnel construction site (Yeoju-si, Korea). As a result, SfM-MVS could generate a point cloud with 20 times higher resolution and double accuracy at 10 times lower cost than LiDAR.

Keywords: SfM (structure-from-motion), MVS (multi-view-stereo), camera settings, UAV flight method, underground digital survey, LiDAR (light-detecting-and-ranging).

1 INTRODUCTION

3D modeling of rock faces has gathered interest during the past decades because it enables safe, remote, and quantitative analysis of various target properties, such as rock mass deformation, joint distribution, and joint roughness (Jiang et al. 2006, Ohnishi et al. 2006, Park & Song 2013, Ge et al. 2017 and Lee et al., 2022). A Point cloud is one of the most widely used forms of 3D modeling, and structure-from-motion & multi-view-stereo (SfM-MVS) technique and light-detecting-and-ranging (LiDAR) technique are the representative methods for generating the point cloud. SfM-MVS gets images photographed at different locations as input and obtains the 3D positions of the image pixels from the parallax between images. Its principle is similar to human eyes, and it has a passive nature that the resultant point cloud quality is highly influenced by the surrounding environment (Baltsavias 1999). LiDAR, in contrast, is an active method that acquires the 3D positions by calculating the time of flight (TOF) of the light ranging from the device. Both methods have pros and cons that the SfM-MVS can generate high-resolution data in a short surveying time even with a cheap consumer-grade

camera while LiDAR can generate high-accuracy data regardless of the illumination. Unmanned-aerial-vehicle (UAV) could be utilized in conjunction with both methods letting faster data acquisition, however, due to the active nature of LiDAR, airborne LiDAR significantly degrades the output quality compared to terrestrial LiDAR (Smith et al. 2016). Although SfM-MVS can survey the target area fast with help of UAVs, it still had a major drawback that the error of the point cloud cannot be predetermined before generation (Ohnishi et al. 2006, Smith et al. 2016 and Eltner et al. 2016) which makes its output in dark environments unreliable since the point cloud quality of SfM-MVS is sensitive to imaging conditions. Also, the absence of instruction for operators on how to photograph the target under various circumstances made SfM-MVS less feasible, therefore, LiDAR has been the dominant tool for generating underground rock face 3D point clouds during the past years (KICT 2017). To overcome the limitation of SfM-MVS and widen its application in underground environments, Leem (2023) has developed a high-performance theoretical error prediction model for SfM-MVS and derived optimum photographing settings, including camera settings (ISO, F number, shutter speed, pixel resolution) and UAV flight method (distance, UAV speed), which minimizes the error under illuminance and time constraints. This work compares the underground rock face 3D modeling performance of both SfM-MVS and terrestrial LiDAR methods with the input images for SfM-MVS captured by a camera on a drone utilizing the optimum camera and UAV flight method derived by the suggested method of Leem (2023).

2 METHODOLOGY

2.1 Site introduction

The two methods were compared at the underground tunnel construction site located in Yeosu-si, Korea. The site was selected for two reasons: insufficient light and the existence of a LiDAR operating survey team. Considering that SfM-MVS has not been commonly used in dark environments due to its passive nature, the site was regarded as an adequate place to check whether the SfM-MVS method is inferior to the LiDAR method in such challenging conditions. Also, there exists a LiDAR operating survey team at the site, so a comparison between SfM-MVS data and actual field LiDAR data of the same target rock face was possible. The total surveying time for both methods was set to 5 mins to imitate the actual surveying procedure conducted at the site.

2.2 Derivation of the optimum photographing settings

This work used the camera mounted on the DJI Mavic 2 Pro drone and the field survey team operated Leica BLK360 imaging laser scanner type LiDAR. Specification of the LiDAR is listed in Table 1 and note that the 3D point accuracy corresponds to the error term of the SfM-MVS generated point cloud clarified in the work of Leem (2023). The difference between the ranging accuracy and the 3D point accuracy is that ranging accuracy only deals with the error in the laser beam direction while 3D point accuracy deals with the error in every direction, which is a more suitable term for rock mass characterization.

Table 1. Leica BLK360 imaging laser scanner specification (<https://leica-geosystems.com/products/laser-scanners/scanners/blk360>).

Field of view (FOV)	360° (horizontal)/300° (vertical)
Range	min 0.6 – up to 60 m
Point measurement rate	up to 360,000 pts/s
Ranging accuracy	4 mm @ 10 m / 7 mm @ 20 m
Measurement speed	Less than 3 mins for complete full dome scan
3D point accuracy	6 mm @ 10m / 8 mm @ 20 m

The optimum photographing settings for the SfM-MVS method are derived by following the optimization procedure suggested by Leem (2023) (Figure 1). The illuminance (E) was measured as 25 lx when utilizing the field lighting which is necessary to comply with the standard safety work guidelines for tunnel construction implemented by the Ministry of Employment and Labor in Korea. The excavation section was roughly about 70 m^2 in size, therefore photographing area per unit time (A) was calculated as $0.5 \text{ m}^2/\text{s}$ by regarding the given time as 4 mins for some tolerance time for drone deceleration. Under the given illuminance and time constraints, we could derive the optimum UAV flight method of distance (D)=3 m and UAV speed (v)=0.2 m/s with consideration of FOV of the camera and optimum camera settings of ISO (S)=3200, F number (N)=2.8, shutter speed (t)=1/40 s, pixel resolution (p)=1920 pixels (FHD). One should aware that the optimum UAV flight method is valid only when the optimum camera settings of the UAV flight method are used together since the minimum achievable errors of the UAV flight methods are coupled with the camera settings in a complex manner.

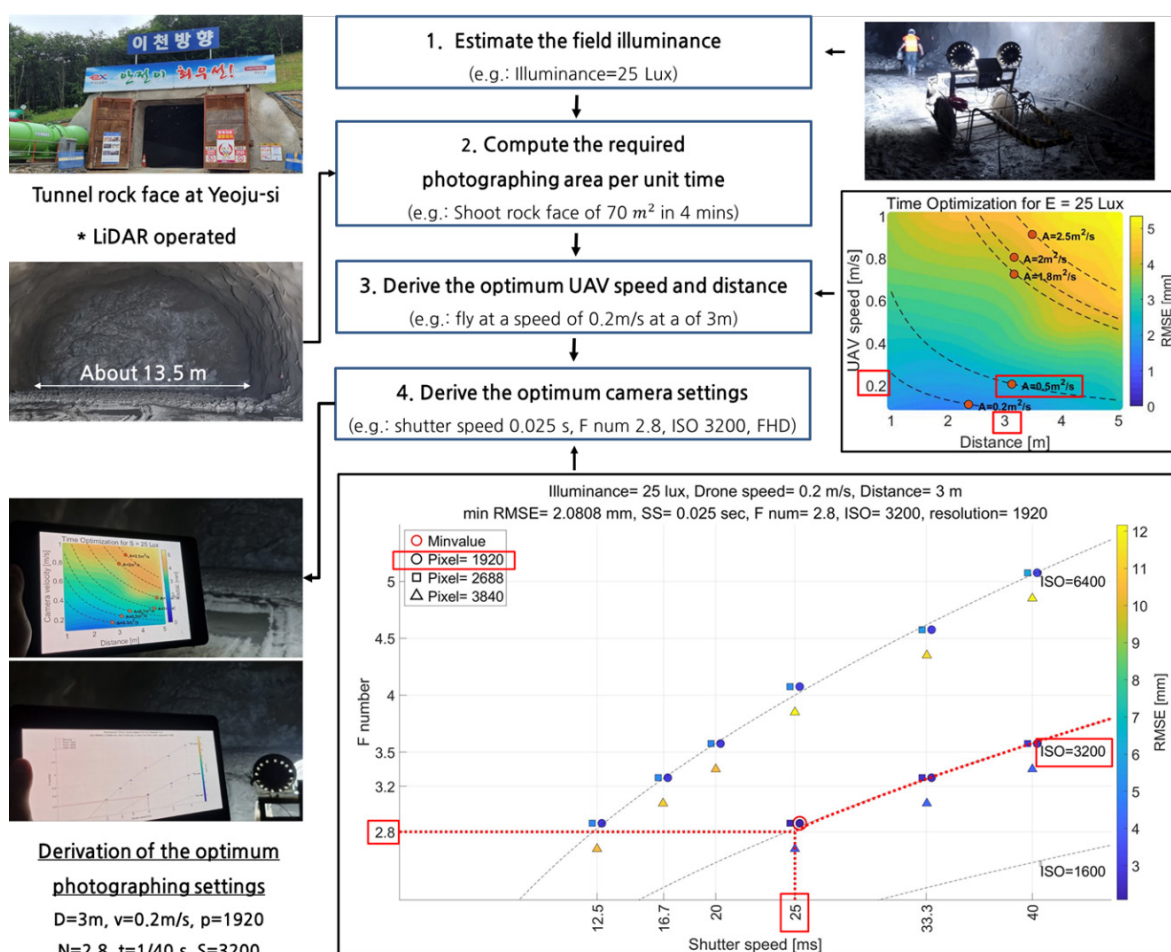


Figure 1. Flow chart of deriving the optimum photographing settings modified from work of Leem (2023) work. When measured illuminance is 25 lx and required photographing area per unit time is $70 \text{ m}^2/4 \text{ mins}$, flying the UAV at $v=0.2 \text{ m/s}$ at $D=3 \text{ m}$ and using camera settings of $N=2.8$, $t=1/40 \text{ s}$, $S=3200$ and $p=1920$ pixels are the optimum photographing settings. The reader should refer to the colored version of this figure.

2.3 Post processing

The input images for SfM-MVS were taken following a parallel axis acquisition scheme (Eltner et al., 2016), using the optimum photographing settings derived above. The SfM-MVS method was implemented using the commercial photogrammetry software developed by Bentley, ContextCapture (<https://www.bentley.com/en/products/brands/contextcapture>), to generate the 3D point cloud from

the photographed images. Then we compared the overall quality of the SfM-MVS generated point cloud and LiDAR generated point cloud, in which the LiDAR data was post-processed to extract the target rock face region by the survey team using the Leica cyclone software (<https://leica-geosystems.com/products/laser-scanners/software/leica-cyclone>).

3 RESULT & DISCUSSION

3.1 Resolution and shadow zone

Figure 2 shows the comparison results of the typical joint plane on the tunnel rock face of the SfM-MVS method and the LiDAR method. The LiDAR-generated point cloud had a low point resolution of roughly 1,700,000 points (equal to 2.43×10^4 pts/m²). Due to the active nature of laser scanning (Baltasvias 1999), intensity data were available, however, it could not express the texture of rock mass well while the texture contains information required for rock mass characterization. Although the instrument was capable of higher point resolution, however, due to the limited time of 5 mins degraded the resolution of the LiDAR-generated point cloud. In contrast, SfM-MVS generated point cloud had a high point resolution of roughly 35,100,000 points (equal to 5.01×10^5 pts/m²) which is about 20 times higher than the LiDAR case. It could well express the texture of the rock mass by reason of SfM-MVS is based on images while it could not obtain intensity data like LiDAR. The passive nature of images (Baltasvias 1999) and the fact that SfM-MVS is based on images allow the SfM-MVS method to obtain high-resolution data from a wide range of areas within a short period. As the survey team used a terrestrial laser scanner (TLS) type LiDAR instrument, shadow zones, where little or no light can reach, were observed because it emits light from a fixed position. Shadow zone did not appear in the SfM-MVS point cloud because images from various locations could be acquired due to the combination with the drone. It should be noted that dark-colored points due to occlusion are different from the shadow zone. Similarly, shadow zones of LiDAR can be expected to be resolved using UAVs, but UAV utilization has been reported to degrade point cloud accuracy and resolution for LiDAR (Smith et al., 2016).

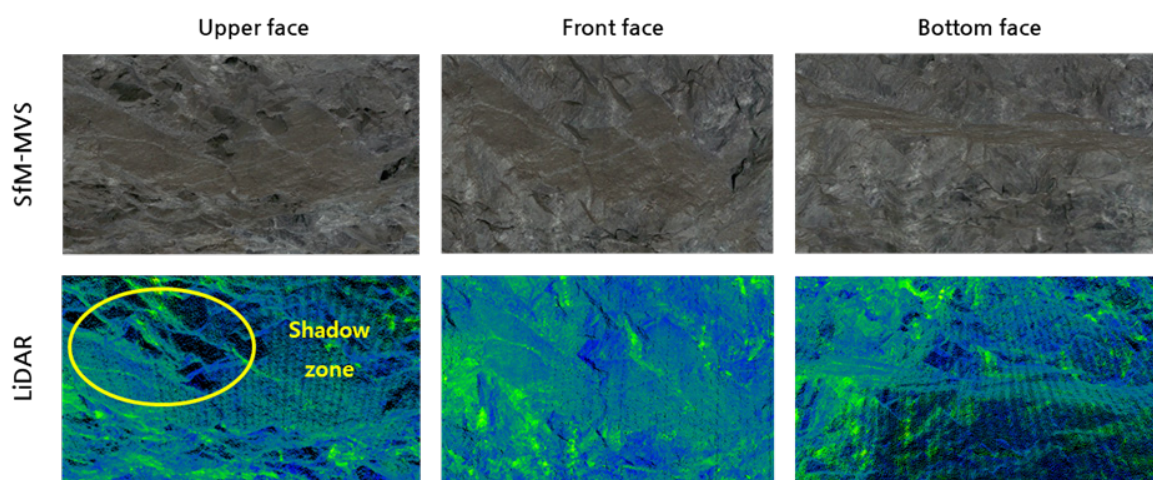


Figure 2. Comparison of the SfM-MVS and the LiDAR generated point cloud. The reader should refer to the colored version of this figure.

3.2 Joint expression capability

Since the joint plane and trace are the important features of rock stability, we qualitatively compared the joint expression capabilities for both methods. In terms of joint plane expression, both methods showed sufficient performance in characterizing the joint plane orientation. However, they had lower point resolutions than the generally used laboratory value of 10^6 (Ge et al. 2017)- 10^8 pts/m² (Park &

Song 2013) for measuring surface roughness purposes, still, LiDAR had more concerns to distort surface roughness than SfM-MVS. For the joint trace expression capability, LiDAR resulted in an overly sparse point cloud to depict the joint traces while SfM-MVS had the ability to express them.

3.3 Accuracy and overall performance

Based on the theoretical error prediction model derived in work of Leem (2023), SfM-MVS utilizing the optimum photographing settings generated a point cloud error of 2 mm under $E=25$ lx and $A=0.5$ m²/s constraints while LiDAR generated a point cloud with error level of 6 mm when measured at a 10 m distance. The overall performance comparison between the two methods is summarized and compared in Table 2 and the comparison shows that the SfM-MVS method could generate a point cloud with 3 times better accuracy and 20 times higher resolution at a cost of 1/9 than the LiDAR method.

Table 2. Summary of performance comparison.

	SfM-MVS	LiDAR
Instrument	DJI Mavic 2 Pro	Leica BLK 360
Capital cost	Approx. 1770 USD	Approx. 15545 USD
Survey time	5 mins	5 mins
Resolution	35,100,000 pts	1,700,000 pts
Accuracy	2 mm (@ $E=25$ lx, $A=0.5$ m ² /s)	6 mm (@ $D=10$ m)
Features	Joints expressed No shadow zones Need of drone control Search process for optimum settings required	Intensity data Shadow zones Terrestrial laser scanner

3.4 Discussion

Numerous studies (Smith & Vericat 2015, Smith et al. 2016 and Eltner et al. 2016) have already stated the outperformance of the SfM-MVS method compared to the LiDAR method in daylight conditions, but this is the first study to our knowledge to confirm such surpass in the underground space. Still, some issues may arise when applying UAV-derived SfM-MVS in underground spaces. For example, extremely poor illuminance conditions may be overcome by attaching lights to drones, but the illuminance in the scene should be kept homogeneous by using lighting that can illuminate a larger area than the FOV of the camera. Also, one should be aware of using such artificial light because images captured under certain frequency light may have periodic noise, which should be avoided by selecting an alternative shutter speed of the camera settings with the expense of slightly higher error (Leem 2023). Similarly, alternative UAV flight methods can be selected in exchange for slightly higher errors if the drone's movement is constrained for reasons such as speed limits or distance limits due to narrow underground spaces. Excessive groundwater flow, such as dripping water from the ceiling, may be problematic because rainy water drops not only blocks the view but also interferes with the drone movement. Fortunately, drones usually have a waterproof function and we have confirmed that our drone could work properly even though the site was quite water dripping condition. For tight survey schedules at underground construction projects, one may shorten the surveying time by operating multiple UAVs simultaneously considering the low price of the instrument.

Our work could confirm the quality of the SfM-MVS generated point cloud and its applicability on rock face 3D modeling in underground space, but the comparison was conducted only for when the SfM-MVS using DJI Mavic 2 Pro camera and Bentley's ContextCapture software and LiDAR method using Leica BLK 360 and Leica cyclone software at the tunnel site in Yeosu-Si, Korea. Future work should therefore include follow-up work on whether the sufficient performance of the SfM-MVS method is still valid with different instruments and software at various underground sites.

4 CONCLUSION

The two methods for rock face 3D point cloud generation, SfM-MVS with optimum photographing settings and LiDAR, are applied and compared at an underground tunnel site in Yeosu-si, Korea where illuminance and survey time are limited. The comparison results show that SfM-MVS generates point cloud with 3 times higher accuracy and 20 times higher resolution than LiDAR at a cost of 1/9. Also, the SfM-MVS point cloud was more favorable in terms of joint plane and trace expression since it had higher accuracy and resolution with additional texture information. The results of this work suggest that SfM-MVS, with optimum photographing settings, can be a powerful tool for 3D modeling rock faces not only at the ground but also underground.

ACKNOWLEDGEMENTS

This work was supported by a grant from the Human Resources Development program (No. 20204010600250) of the Korea Institute of Energy Technology Evaluation and Planning (KETEP), funded by the Ministry of Trade, Industry, and Energy of the Korean Government, and also by the Energy & Mineral Resources Development Association of Korea (EMRD) grant funded by the Korea government (MOTIE) (2021060003, Training Program for Specialists in Smart Mining).

REFERENCES

- Baltsavias, E. P. 1999. A comparison between photogrammetry and laser scanning. *ISPRS Journal of photogrammetry and Remote Sensing* 54 (2-3), pp. 83-94.
- Eltner, A., Kaiser, A., Castillo, C., Rock, G., Neugirg, F., & Abellán, A. 2016. Image-based surface reconstruction in geomorphometry—merits, limits and developments. *Earth Surface Dynamics* 4 (2), pp. 359-389.
- Ge, Y., Tang, H., Ez Eldin, M. A. M., Wang, L., Wu, Q., & Xiong, C. 2017. Evolution process of natural rock joint roughness during direct shear tests. *International Journal of Geomechanics* 17 (5), pp. E4016013.
- Jiang, Y., Li, B., & Tanabashi, Y. 2006. Estimating the relation between surface roughness and mechanical properties of rock joints. *International Journal of Rock Mechanics and Mining Sciences* 43 (6), pp. 837-846.
- KICT. 2017. *Tunnelsigong jung digital mappingeul tonghan online ampanjeong gisul mit unyeongmodel gaebal choejongbogoseo [Final Report on the Development of Online Rock Mass Classification Technology and Operation Model through Digital Mapping in Tunnel Construction]*. National Library of Korea (3), pp. 1-578.
- Lee, Y. K., Kim, J., Choi, C. S., & Song, J. J. 2022. Semi-automatic calculation of joint trace length from digital images based on deep learning and data structuring techniques. *International Journal of Rock Mechanics and Mining Sciences* 149, pp. 104981.
- Leem, J.S. 2023. *Camera settings and flight method for optimum photography of UAV based SfM-MVS*. Master's thesis. Seoul National University. Korea.
- Ohnishi, Y., Nishiyama, S., Yano, T., Matsuyama, H., & Amano, K. 2006. A study of the application of digital photogrammetry to slope monitoring systems. *International Journal of Rock Mechanics and Mining Sciences* 43 (5), pp. 756-766.
- Park, J. W., & Song, J. J. 2013. Numerical method for the determination of contact areas of a rock joint under normal and shear loads. *International Journal of Rock Mechanics and Mining Sciences* 58, pp. 8-22.
- Smith, M. W., & Vericat, D. 2015. From experimental plots to experimental landscapes: topography, erosion and deposition in sub-humid badlands from structure-from-motion photogrammetry. *Earth Surface Processes and Landforms* 40 (12), pp. 1656-1671.
- Smith, M. W., Carrivick, J. L., & Quincey, D. J. 2016. Structure from motion photogrammetry in physical geography. *Progress in physical geography* 40 (2), pp. 247-275.